Limnol. Oceanogr., 49(5), 2004, 1630–1641

Gas transfer velocities of CO_2 in three European estuaries (Randers Fjord, Scheldt, and Thames)

Alberto Vieira Borges,[1] *Bruno Delille, and Laure-Sophie Schiettecatte*
Université de Liège, Interfacultary Center for Marine Resarch, Unité d'Océanographie Chimique, Institut de Physique (B5), B-4000 Liège, Belgium

Frédéric Gazeau
Université de Liège, Interfacultary Center for Marine Resarch, Unité d'Océanographie Chimique, Institut de Physique (B5), B-4000 Liège, Belgium; Laboratoire d'Océanographie de Villefranche, Université de Paris 6, BP 28, F-06234 Villefranche-sur-mer, France

Gwenaël Abril
Université de Bordeaux 1, Département de Géologie et Océanographie, Environnements et Paléoenvironnements Océaniques, Avenue des Facultés, F-33405 Talence, France

Michel Frankignoulle
Université de Liège, Interfacultary Center for Marine Resarch, Unité d'Océanographie Chimique, Institut de Physique (B5), B-4000 Liège, Belgium

Abstract

We measured the flux of CO_2 across the air–water interface using the floating chamber method in three European estuaries with contrasting physical characteristics (Randers Fjord, Scheldt, and Thames). We computed the gas transfer velocity of CO_2 (k) from the CO_2 flux and concomitant measurements of the air–water gradient of the partial pressure of CO_2 (pCO_2). There was a significant linear relationship between k and wind speed for each of the three estuaries. The differences of the y-intercept and the slope between the three sites are related to differences in the contribution of tidal currents to water turbulence at the interface and fetch limitation. The contribution to k from turbulence generated by tidal currents is negligible in microtidal estuaries such as Randers Fjord but is substantial, at low to moderate wind speeds, in macrotidal estuaries such as the Scheldt and the Thames. Our results clearly show that in estuaries a simple parameterization of k as a function of wind speed is site specific and strongly suggest that the y-intercept of the linear relationship is mostly influenced by the contribution of tidal currents, whereas the slope is influenced by fetch limitation. This implies that substantial errors in flux computations are incurred if generic relationships of the gas transfer velocity as a function of wind speed are employed in estuarine environments for the purpose of biogas air–water flux budgets and ecosystem metabolic studies.

Based on organic carbon flux budgets, the overall picture of the net ecosystem metabolism in the coastal ocean is that temperate open continental shelves (bordered by a continental margin) are net autotrophic (net exporters of carbon and thus potential sinks for atmospheric CO_2) while near-shore systems influenced by anthropogenic and/or terrestrial organic carbon inputs, in particular temperate estuaries, are net heterotrophic (e.g., Smith and Mackenzie 1987; Gattuso et al. 1998). This picture has recently been confirmed by direct measurements of the air–water gradient of pCO_2 with a sufficient temporal and spatial resolution to allow the annual integration of the computed air–water CO_2 fluxes. Temperate open continental shelves are net sinks for atmospheric CO_2 (e.g., Tsunogai et al. 1999; Frankignoulle and Borges 2001*a*; Borges and Frankignoulle 2002*a*; DeGranpre et al. 2002), while temperate estuaries are net sources of CO_2 to the atmosphere (e.g. Frankignoulle et al. 1998; Cai et al. 2000; Raymond et al. 2000; Borges and Frankignoulle 2002*b*). Although the surface area of estuaries is globally about 20 times smaller than that of open continental shelves, the air–water fluxes of CO_2 in the temperate estuaries so far studied are about two orders of magnitude higher (about $+100$ mmol m^{-2} d^{-1}) than over temperate open continental shelves (about -5 mmol m^{-2} d^{-1}). A global integration of the CO_2 fluxes in these two systems is not possible at present time because of the lack of adequate data coverage. Indeed, few data are

[1] Corresponding author (Alberto.Borges@ulg.ac.be).

Acknowledgments

We thank the crew of the R. V. *Belgica* for full collaboration during the Scheldt and Thames cruises, Niels Iversen for welcome on the Randers Fjord, Management Unit of the North Sea Mathematical Models for providing thermosalinograph and meteorological data during the Scheldt and Thames cruises, Renzo Biondo, Emile Libert, and Jean-Marie Théate for invaluable technical support, and an anonymous reviewer and J. N. Kremer for constructive comments on a previous version of the paper. This work was funded by the European Union through the BIOGEST (ENV4-CT96-0213) and EUROTROPH (EVK3-CT-2000-00040) projects, and by the Fonds National de la Recherche Scientifique (FRFC 2.4545.02) where A.V.B and M.F. are, respectively, a postdoctoral researcher and a senior research associate. This is MARE contribution 043.

Table 1. Basic data of the three studied sites. The surface area, length, and width are for the region of salinity mixing (the tidal freshwater region is excluded). The average estuary depth is at low tide and for the region of salinity mixing; however, note that measurements were made in the navigation channel.

	Randers Fjord	Thames	Scheldt
Type	microtidal	macrotidal	macrotidal
Catchment area (10^3 km^2)	3.3	14	21
Surface area (km^2)	22	215	268
Length (km)	27	85	75
Width (km)	1.0	2.1	3.3
Average depth (m)	2	8	10
Navigation channel depth (m)	7	12	13
Tidal amplitude (m)	0.1–0.2	3–6	2–5
Fresh water discharge (km^3 yr^{-1})	1.2	9.5	3.8
Residence time (days)	5–10	20–40	30–90

available at subtropical and tropical latitudes in both estuaries and continental shelves. The recent work by Cai et al. (2003) in the U.S. South Atlantic Bight shows that, unlike temperate continental shelves, subtropical continental shelves could in general be sources of CO_2. However, regional comparisons strongly suggest that CO_2 fluxes in estuaries could be very significant. For instance, the integrated emission of atmospheric CO_2 from Europe's estuaries (30 to 60×10^9 kg C yr^{-1}; Frankignoulle et al. 1998) is of the same order of magnitude as the integrated sink over the European open continental shelf (90 to 170×10^9 kg C yr^{-1}, Frankignoulle and Borges 2001*a*). Thus, more data of pCO_2 in estuaries and continental shelves are needed worldwide to allow the computation and global integration of the related air–water CO_2 fluxes. This also requires a better constraint on the formulation of the gas transfer velocity, which is the subject of a long-lived debate that at present time seems unresolved in both open oceanic waters (e.g., Liss and Merlivat 1986; Wanninkhof 1992; Jacobs et al. 1999; Wanninkhof and McGillis 1999; Nightingale et al. 2000; McGillis et al. 2001) and estuarine environments (e.g., Raymond and Cole 2001; Kremer et al. 2003*a*). Finally, the computation of gas exchange is also critical in the study of ecosystem metabolism based on the open-water method using O_2 and dissolved inorganic carbon measurements (e.g., Smith and Key 1975; Kremer et al. 2003*a*).

The flux of CO_2 across the air–water interface can be computed according to

$$F = \varepsilon k \alpha \Delta pCO_2 \quad (1)$$

where α is the solubility coefficient of CO_2, ΔpCO_2 is the air–water gradient of pCO_2, k is the gas transfer velocity of CO_2 (also referred to as piston velocity), and ε is the chemical enhancement factor of gas exchange.

In both open oceanic and coastal environments, highly precise and accurate methods to measure ΔpCO_2 are available; thus, the largest uncertainty in the computation of F comes from the k term (α is straightforwardly computed from salinity and water temperature, and the contribution from ε is usually negligible, except under very low turbulent conditions, see, e.g., Wanninkhof 1992 for open oceanic waters and Raymond and Cole 2001 for estuarine environments). Based on numerous theoretical, laboratory, and field studies, it is well established that k depends on a variety of variables such as capillary and breaking waves, boundary layer stability, air bubbles, surfactant surface films, evaporation/condensation, and precipitation, but the most important one is turbulence at the air–water interface (in the case of sparingly soluble gases such as CO_2 the critical variable is turbulence in the liquid phase). In open oceanic waters, the gas transfer velocity of CO_2 is usually parameterized as a function of wind speed because wind stress is the main generator of turbulence in these systems.

In a recent review that compiles available measurements of k based on different methodologies in various estuaries, Raymond and Cole (2001) suggested that the parameterization of k as a function of wind speed could be significantly different in estuarine environments from those developed in open oceanic waters (higher values of k in estuaries for the same wind speed). To contribute to the debate, we analyze in the present paper a reasonably large data set of k values, based on the floating chamber method, in three European estuaries with contrasting physical characteristics (Randers Fjord, Denmark; Scheldt, Belgium/the Netherlands; and Thames, United Kingdom).

Materials and methods

Pertinent characteristics of the three studied estuaries are summarized in Table 1. During the Thames and the Scheldt cruises, sampling was carried out to cover the full salinity range, typically by steps of 2.5 of salinity. During the Scheldt cruise of November 2002, four stations (51.13°N 4.31°E, 51.23°N 4.40°E, 51.41°N 4.04°E, 51.39°N 4.21°E) were occupied for 24 h and flux measurements were carried out approximately every 10 min during daytime (10 h). During the Randers Fjord cruises, three stations (56.46°N 10.04°E, 56.62°N 10.23°E, 56.61°N 10.30°E) were occupied for 24 h and flux measurements were carried out hourly.

During the Thames cruises and most of the Scheldt cruises (Table 2), pCO_2 was computed from the measurements of pH and total alkalinity (TAlk) sampled from a Niskin bottle in subsurface water. During the three most recent Scheldt cruises (Table 2), pCO_2 was measured directly (1-min recording interval) with an infrared gas analyzer (IRGA, Licor Li-6262) in air equilibrated with subsurface water (pumped from a depth of 2.5 m), using the equilibrator described by

Table 2. Sampling dates and range of variables (salinity, water pCO_2 [ppm]; atmospheric pCO_2 [ppm]; air–water CO_2 fluxes [mmol m^{-2} d^{-1}]) during the cruises carried out in the three studied estuaries. *n*, total number of air–water CO_2 flux measurements.

	Salinity	pCO_{2water}	pCO_{2air}	Air–water CO_2 flux	*n*	*n**
Randers Fjord						
25 Apr–29 Apr 2001	2–19	206–1011 (FES)	370–400	−36–65	27	10
20 Aug–28 Aug 2001	0–21	370–3910 (FES)	355–435	0–290	66	46
Scheldt						
27 Nov–29 Nov 1995	1–29	605–6800 (pH/TAlk)	362–455	63–850	36	36
08 Jul–12 Jul 1996	1–30	472–7170 (pH/TAlk)	365–401	43–1465	48	45
09 Dec–13 Dec 1996	0–30	608–5632 (pH/TAlk)	349–390	23–740	42	42
25 May–28 May 1998	1–30	299–7718 (pH/TAlk)	392–460	−21–767	34	22
05 Oct–08 Oct 1998	0–27	956–7741 (pH/TAlk)	414–458	104–2270	34	34
04 Jul–06 Jul 2000	1–31	523–8351 (Eq)	387–445	15–1178	24	21
06 Nov–08 Nov 2000	0–20	614–5512 (Eq)	401–455	92–1328	12	10
06 Nov–12 Nov 2002	0–17	993–7553 (Eq)	368–422	66–2028	112	112
Thames						
11 Sep–18 Sep 1996	2–35	458–4617 (pH/TAlk)	404–457	41–1728	58	55
16 Feb-18 Feb 1999	0–33	281–3025 (pH/TAlk)	400–460	0–1587	34	26

*n**, number of flux measurements for an absolute air–water pCO_2 gradient > 200 ppm; FES = pCO_2 measurements carried out with the floating equilibrator system; Eq = pCO_2 measurements carried out with an equilibrator from the subsurface water supply of the *R/V Belgica*; pH/TAlk = pCO_2 computed from the measurements of pH and TAlk sampled from a Niskin bottle in subsurface waters (*see Materials and methods for details*).

Frankignoulle et al. (2001). During the Randers Fjord cruises, pCO_2 was measured directly by equilibration with the floating equilibrator system (FES) described by Frankignoulle et al. (2003). In brief, the FES is a buoy containing an equilibrator, an IRGA, water and air temperature probes, an anemometer, and a data logger (1-min recording interval), powered by four 12-volt batteries and a solar panel, providing an autonomy up to 30 h. For a detailed description of the pH and TAlk measurement methods, the computations of pCO_2 from pH and TAlk and the calibration procedure of the IRGA refer to Frankignoulle and Borges (2001*b*). Note that the measurements of pCO_2 by equilibration and the computed values of pCO_2 from pH and TAlk are consistent within $\pm 1.5\%$ (Frankignoulle and Borges 2001*b*).

The air–water CO_2 fluxes were measured with the floating chamber method described by Frankignoulle (1988) from a drifting rubber boat to avoid the interference of water turbulence within the chamber created by passing water current observed in earlier measurements carried out from a fixed point (Frankignoulle unpubl. data). The chamber is a plastic right circular cone (top radius = 49 cm; bottom radius = 57 cm; height = 28 cm) mounted on a float and connected to a closed air circuit with an air pump (3 L min^{-1}) and an IRGA, both powered with a 12-volt battery. The IRGA was calibrated daily using pure nitrogen (Air Liquide Belgium) and a gas mixture with a CO_2 molar fraction of 351 ppm (Air Liquide Belgium). The readings of pCO_2 in the chamber were written down every 30 s during 5 min in the Scheldt and Thames estuaries and during 10 min in the Randers Fjord because in the latter the flux signal was weaker than in the former two estuaries (*see Table 2*). The flux was computed from the slope of the linear regression of pCO_2 against time (r^2 usually ≥ 0.99) according to Frankignoulle (1988). The uncertainty of the flux computation due to SE on the regression slope is on average $\pm 3\%$.

The floating chamber technique has been dismissed by several workers (Liss and Merlivat 1986; Raymond and Cole 2001), and one of the critiques of this technique is that the chamber covers the water surface and eliminates wind stress. However, for sparingly soluble gases such as CO_2, gas transfer is controlled by turbulence in the liquid phase. Thus, if the floating chamber does not disrupt the underlying water turbulence, then the corresponding gas transfer measurements should be reasonable estimates of those from the undisturbed surface. The disturbance of the floating chamber on the surface wind boundary layer was tested experimentally by Kremer et al. (2003*b*). They measured O_2 fluxes using a floating chamber with an adjustable speed fan to generate air turbulence and using a control floating chamber in parallel. Under moderate wind conditions, the additional air turbulence from the fan only increased the fluxes by 2% to 12% compared to the control chamber. Kremer et al. (2003*b*) also report a series of experiments comparing the floating chamber technique with mass balance approaches of O_2, ^{222}Rn, and ^{3}He in various experimental settings (laboratory tanks, outdoor tanks, mesocosms, and lakes). Fluxes based on the floating chamber technique agreed with the other direct methods within 10% to 30%. However, two publications report large discrepancies between the floating chamber technique and other approaches (Belanger and Korzum 1991; Matthews et al. 2003) that, in our opinion, highlight the limits of the method rather than dismiss it altogether. Belanger and Korzum (1991) compared O_2 evasion rates from pools by a mass balance approach and floating chamber measurements. They concluded that the floating chamber measurements were biased by changes of temperature and pressure during the experiments. However, the duration of these measurements was several hours and temperature and pressure changes are not expected to interfere during very short deployments of the floating chamber (such

as in our case). Matthews et al. (2003) compared *k* estimates in a small sheltered boreal reservoir, based on floating chamber and SF_6 evasion techniques. However, during their experiment, wind speeds were extremely low, on average 0.2 m s^{-1} and never exceeding 0.5 m s^{-1}. As noted by Kremer et al. (2003*b*), the fluxes measured in nearly motionless waters with a floating chamber should be taken with caution. Also, estuarine environments (such as in our case) are much more turbulent because of tidal currents than the reservoir studied by Matthews et al. (2003). Finally, an indirect validation of this technique is given by Frankignoulle et al. (1996), who showed that floating chamber measurements over several coral reef systems give *k* estimates that fall between those based on the empirical formulations of Liss and Merlivat (1986) and Wanninkhof (1992).

The gas transfer velocity of CO_2 was computed from the CO_2 flux and ΔpCO_2 measurements (atmospheric pCO_2 was measured and recorded at the start of each flux measurement), using the CO_2 solubility coefficient formulated by Weiss (1974) and normalized to a Schmidt number (Sc) of 600 (k_{600}), assuming a dependency of the gas transfer velocity proportional to $Sc^{-0.5}$. Estuaries are highly turbulent systems (*see Discussion*), and the dependency of *k* proportional to $Sc^{-2/3}$ usually applied in open oceanic waters for the smooth surface regime, i.e., at wind speeds below 3 m s^{-1} (e.g., Liss and Merlivat 1986), probably does not hold true. The Schmidt number was computed for a given salinity from the formulations for salinity 0 and 35 given by Wanninkhof (1992) and assuming that Sc varies linearly with salinity.

During the Thames and Scheldt cruises, wind speed was measured at 18 m height with a Friedrichs 4034.000 BG cup anemometer and recorded every 10 s. During the Randers Fjord cruises, wind speed measurements at 2 m height from a Young 03002VP cup anemometer were recorded every 60 s. The winds speeds were referenced to a height of 10 m (u_{10}) according to Smith (1988) using concomitant air and water temperature measurements and were averaged for the period of each flux measurement. Water current speeds in subsurface waters were measured with an Aanderaa RCM7 and were recorded every minute during the Randers Fjord cruises and the November 2002 Scheldt cruise and were averaged for the period of each flux measurement.

Results

During all cruises and in the three estuaries, the full gradient of salinity was sampled (Table 2), except during the November 2000 Scheldt cruise because of bad weather conditions and during the November 2002 Scheldt cruise because of a different sampling strategy (*see Materials and methods*). The range of water pCO_2 values spans one order of magnitude and is highest in the Scheldt estuary, although variable from one cruise to another. Oversaturation of CO_2 with respect to atmospheric equilibrium is observed in all three estuaries, although significant undersaturations are observed on some occasions, systematically in the high-salinity region of the estuary (Randers Fjord in April, Scheldt in May, and Thames in February) (Table 2). The range of CO_2 air–water fluxes spans two orders of magnitude and is smaller in the Randers Fjord, while the Scheldt and the Thames show similar ranges. The atmospheric pCO_2 values are above typical global average values, as observed in other nearshore coastal systems (e.g., Bakker et al. 1996; Borges and Frankignoulle 2001). Indeed, atmospheric pCO_2 values in the Randers Fjord, Scheldt, and Thames are on average 3 (±14 SD), 27 (±22 SD), and 42 (±11 SD) parts per million (ppm) above the ''uncontaminated'' values from Weather Station Mike (66.00°N 2.00°E), representative of the open North Sea waters (from the National Oceanic and Atmospheric Administration Climate Monitoring and Diagnostics Laboratory air samples network, available on the internet at http://www.cmdl.noaa.gov/). The individual atmospheric pCO_2 values for each cruise were compared with the corresponding monthly value at Weather Station Mike, where from 1995 to 2002 the annual mean increased from 361 to 373 ppm.

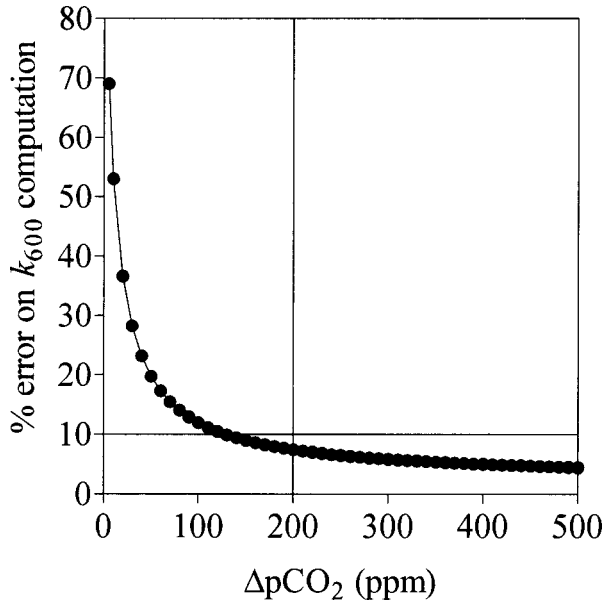

Fig. 1. Theoretical error (±%) on the computation of the gas transfer velocity of CO_2 (k_{600}) as a function of the air–water gradient of CO_2 (ΔpCO_2 in ppm), assuming a constant uncertainty on ΔpCO_2 of ±3%.

The k_{600} data sets were filtered before further analysis because as ΔpCO_2 values approach zero, the computation of k_{600} becomes more sensitive to error. This was investigated by assuming a reasonable error on ΔpCO_2 of ±3% and then assessing the corresponding error on the computation of k_{600} (Fig. 1). An absolute value of ΔpCO_2 equal to 200 ppm was chosen as the threshold value below which the k_{600} data were rejected because it corresponds to a good compromise between an acceptable error on the k_{600} computation (below ±10%, Fig. 1) and maintains a fairly large number of filtered variables. After this filtering, the remaining k_{600} data sets correspond to 60%, 88%, and 94% of the original data sets for the Randers Fjord, Thames, and Scheldt, respectively (Table 2). The k_{600} data were averaged over wind speed bins of 2 m s^{-1}, a common practice in gas transfer velocity studies (e.g., Cole and Caraco 1998; Fairall et al. 2000; McGillis et al. 2001), but one that changes the statistical power of regression and hypothesis testing. A rather large interval of

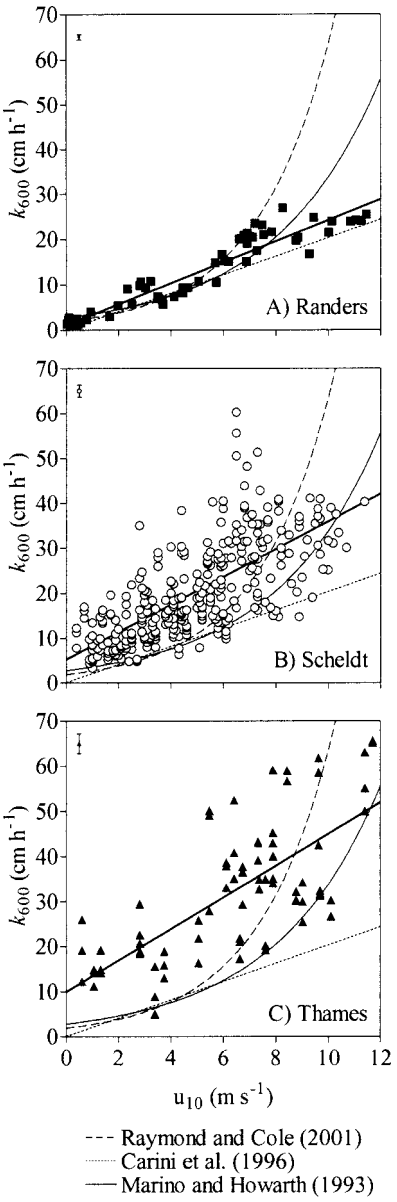

Fig. 2. Gas transfer velocity of CO_2 (k_{600}, cm h^{-1}) as a function of wind speed at 10 m height (u_{10}, m s^{-1}) in the three studied estuaries and three published relationships. The error bars on the top left corner of the plot correspond, for each of the three estuaries, to the average uncertainty on k_{600} estimated using the individual standard error on the slope of the regression of pCO_2 in the floating chamber against time (from which the CO_2 flux was computed; *see the Materials and methods section*) and assuming an error on ΔpCO_2 of ±3%. The estimated uncertainty on k_{600} varies with wind speed; in the Thames and Scheldt it ranges from about ±1 to ±4 cm h^{-1} at, respectively, low and high wind speeds; in the Randers Fjord it ranges from about ±0.1 to ±1.4 cm h^{-1} at, respectively, low and high wind speeds. The solid bold line corresponds to model 1 regression functions (Table 3). The Raymond and Cole (2001) relationship (k_{600} = 1.91 exp [0.35u_{10}]) is based on a compilation of published k_{600} values in various rivers and estuaries and obtained using different methodologies (floating chamber, natural tracers [CFC, ^{222}Rn] and purposeful tracer [SF_6]). The Carini et al. (1996) relationship (k_{600} = 0.045 + 2.0277u_{10}) is based on a SF_6 release experiment in the Parker River estuary. The Marino and Howarth (1993) relationship (k_{600} = 0.94 exp [1.09 + 0.249u_{10}]) is based on floating chamber oxygen measurements in the tidal freshwater portion of the Hudson River estuary. The latter two relationships were developed for oxygen and are expressed as k_{600} using the Schmidt number formulations given by Wanninkhof (1992) and assuming a dependency of the gas transfer velocity proportional to Sc$^{-0.5}$.

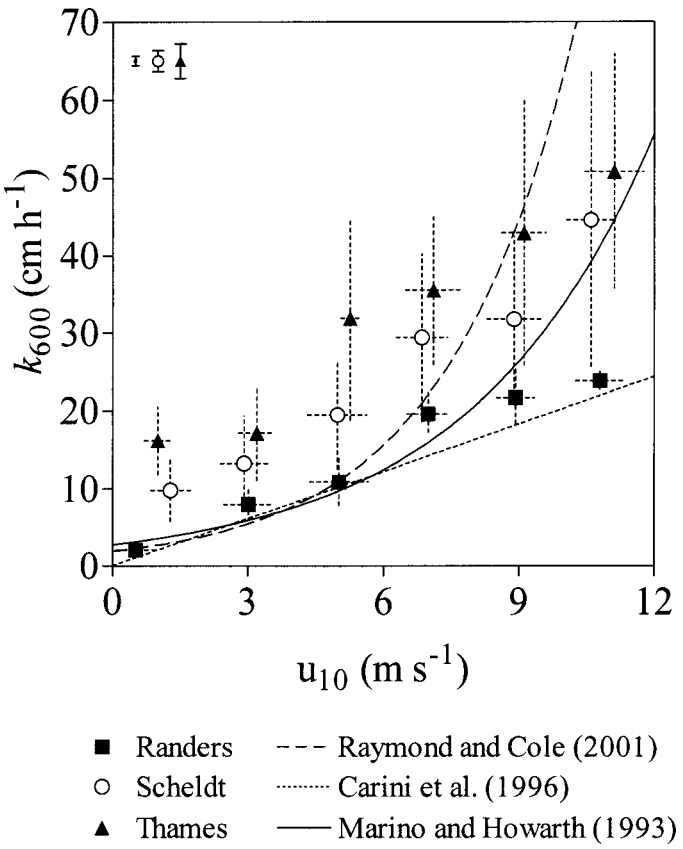

Fig. 3. Gas transfer velocity of CO_2 (k_{600}, cm h^{-1}) as a function of wind speed at 10 m height (u_{10}, m s^{-1}) in the three studied estuaries and three published relationships. The data were averaged over wind speed bins of 2 m s^{-1}. Standard deviations are shown by the horizontal and vertical dotted lines for the bin averages of u_{10} and k_{600}, respectively. The error bars on the top left corner of the plot correspond, for each of the three estuaries, to the average uncertainty on the k_{600} (refer to legend of Fig. 2 for details). The long-dashed line corresponds to the Raymond and Cole (2001) relationship, the short-dashed line corresponds to the Carini et al. (1996) relationship, and the solid line corresponds to the Marino and Howarth (1993) relationship (refer to legend of Fig. 2 for details).

wind speed bins was chosen because the data sets for the Randers Fjord and Thames are small compared to the one for the Scheldt (Table 2).

Figure 2 shows unbinned k_{600} versus wind speed in the Randers Fjord, the Scheldt, and the Thames. In the three estuaries, a distinct increasing trend of k_{600} values with wind speed is observed, although in the macrotidal Scheldt and Thames estuaries, data show higher scatter than the microtidal Randers Fjord. Note that the average estimated uncer-

Table 3. Linear regression functions between the gas transfer velocity of CO_2 (k_{600}, cm h^{-1}) and wind speed at 10-m height (u_{10}, m s^{-1}) in the three studied estuaries, based on unbinned and bin-averaged data (k_{600} data were averaged over wind speed bins of 2 m s^{-1}).*

	$k_{600} = a\ (\pm SE) + b\ (\pm SE)u_{10}$	r^2	p	n
Unbinned data				
Scheldt	$k_{600} = 3.8(\pm 1.0) + 3.45(\pm 0.19)u_{10}$	0.519	<0.0001	322
Thames	$k_{600} = 9.7(\pm 3.2) + 3.64(\pm 0.45)u_{10}$	0.471	<0.0001	76
Randers Fjord	$k_{600} = 1.2(\pm 0.7) + 2.30(\pm 0.11)u_{10}$	0.897	<0.0001	56
Bin-averaged data				
Scheldt	$k_{600} = 3.4(\pm 2.4) + 3.60(\pm 0.35)u_{10}$	0.963	0.0005	6
Thames	$k_{600} = 10.2(\pm 2.4) + 3.62(\pm 0.35)u_{10}$	0.965	0.0005	6
Randers Fjord	$k_{600} = 0.9(\pm 1.5) + 2.30(\pm 0.22)u_{10}$	0.965	0.0004	6

* These relationships are only valid for u_{10} spanning the range of values between 0 and 11 m s^{-1}. For unbinned data, the regression function was computed with model 1 least squares fit. For bin-averaged data, the regression function was computed with model 2 functional fit. For the Scheldt and Thames regression functions, the slopes are not statistically different ($p = 0.6299$ for unbinned data; $p = 0.9675$ for bin-averaged data) but the y-intercepts are statistically different ($p < 0.0001$ for unbinned data; $p = 0.0016$ for bin-averaged data). The slope of the regression function of the Randers Fjord is statistically different from those of the Scheldt ($p = 0.0016$ for unbinned data; $p = 0.0099$ for bin-averaged data) and the Thames ($p = 0.0086$ for unbinned data; $p = 0.0090$ for bin-averaged data).

tainty on the k_{600} values (error bars on top left corner of plots in Fig. 2) is lower than the data scatter. For wind speeds below 6 m s^{-1}, the k_{600} values in the Randers Fjord follow published parameterizations in estuaries of k as a function of wind speed. For wind speed above 6 m s^{-1}, the k_{600} values in the Randers roughly follow the Carini et al. (1996) parameterization. For wind speeds below 8 m s^{-1}, the lowest k_{600} values in the Scheldt and Thames for a given wind speed fall on the lines from published parameterizations. However, the highest k_{600} values at a given wind speed are about eight times higher than the observed minimal values. This suggests that at a given wind speed, a process other than wind stress increases k_{600} in the Scheldt and Thames. Figure 3 shows the averaged k_{600} over wind speed bins of 2 m s^{-1} versus wind speed in the three estuaries. The binned k_{600} values are highly variable from one estuary to another, and at a given wind speed the highest values are observed in the Thames and the lowest in the Randers Fjord. The ratio of binned k_{600} values between the estuaries varies with wind speed; at low wind speeds, k_{600} is about eight times higher and at high wind speeds about two times higher in the Thames than in the Randers Fjord.

The k_{600} was parameterized as a function of wind speed by linear regression in each of the three studied estuaries (Table 3). Although various parameterization functions have been used in literature (linear, e.g., Liss and Merlivat 1986; Carini et al. 1996; Kremer et al. 2003*a*; power law, e.g., Hartman and Hammond 1985; Wanninkhof 1992; Cole and Caraco 1998; Jacobs et al. 1999; Wanninkhof and McGillis 1999; Nightingale et al. 2000; McGillis et al. 2001; exponential, e.g., Marino and Howarth 1993; Raymond and Cole 2001; Kremer et al. 2003*a*), the linear model is clearly appropriate for Randers Fjord, and for the Scheldt and Thames estuaries the linear approximation is the best first approximation especially considering the scatter. Moreover, in wind tunnel experiments, k has been shown to vary linearly with wind speed between 2 and 13 m s^{-1} (Broecker and Siems 1984), the range of our data. In wind tunnel experiments, at wind speeds above 13 m s^{-1}, the slope of k versus wind speed increased because of presence of air bubbles from breaking waves. Kremer et al. (2003*a*) also showed that a linear relationship between k and wind speed provides the best data fit in Sage Lot Pond and Childs River estuaries (Waquoit Bay).

The model 2 regression functions of binned k_{600} and model 1 regression functions of unbinned k_{600} versus wind speed are highly significant in the three studied estuaries (Table 3). The slopes and y-intercepts of unbinned and binned k_{600} versus wind speed relationships in the three estuaries (model 1 and 2 functions, respectively) are not significantly different (Table 3). The slopes of the linear regression functions are similar in the Scheldt and the Thames and significantly higher than the one in the Randers Fjord. The y-intercept of the linear regression function in the Thames is higher than those of the Randers Fjord and the Scheldt.

Discussion

The differences of the y-intercept and slope of the linear regressions of k_{600} as a function of wind speed described in the previous section for the three studied estuaries are discussed in relation to the potential contribution of water currents to water turbulence and fetch limitation.

Contribution of water currents to k_{600}—In the macrotidal Scheldt and Thames estuaries k_{600} values showed high scatter, and at wind speeds below 8 m s^{-1} most k_{600} values are above the values predicted by published parameterizations (Fig. 2). In contrast, in the microtidal Randers Fjord k_{600} values showed much lesser scatter. This strongly suggests that, in the Scheldt and Thames, tidal currents, in addition to wind stress, significantly contribute to k_{600} and induce high variability depending on the tidal phase (maximum ebb or flow and tidal slacks).

In streams, the interaction of the gravity flow and bottom topography generates turbulence because of bottom shear that is frequently considered to be the main factor controlling the gas transfer velocity of sparingly soluble gases in these sheltered systems where wind is usually very low. This has led to various parameterizations of the gas transfer velocity

as a function of water current and depth based on empirical or conceptual approaches, reviewed by Bansal (1973) and more recently by Melching and Flores (1999) and Gualtieri et al. (2002). In estuaries, the tidal current can be as high as the gravity flow in streams and, thus, could in theory contribute significantly to k_{600}. To our best knowledge, in estuaries, this has been investigated in the field by Hartman and Hammond (1984) in San Francisco Bay using floating chamber ^{222}Rn measurements and by Zappa et al. (2003) in Plum Island Sound using the gradient flux technique. Hartman and Hammond (1984) found no distinct evidence for the contribution of water currents to the gas transfer velocity. However, in this study water currents were estimated from tide tables and not actually measured. Moreover, the sampling period for each flux measurement was rather long (1 h) in comparison with the time-scale characteristic of tidal current variability. Zappa et al. (2003) carried out four k measurements under low winds (1.9 m s^{-1}) during half a tidal cycle and found a significant enhancement of k (up to 10 cm h^{-1}) related to water currents measured with an acoustic Doppler current profiler (ranging from 10 to 80 cm s^{-1}).

Water currents measurements concomitant to flux measurements were obtained during the two Randers Fjord cruises and the November 2002 Scheldt cruise. Although water currents are expected to contribute to water turbulence whatever the wind speed, their effect is best identified if the contribution to turbulence from wind stress is low ($u_{10} < 4$ m s^{-1}). In the Randers Fjord, water current concomitant to flux measurements at wind speeds below 4 m s^{-1} ranged from 1 to 38 cm s^{-1} (on average 11 ± 12 SD cm s^{-1}). So it is possible to compare quantitatively water currents to the corresponding k_{600} values. In contrast, during the November 2002 Scheldt cruise, current speeds were systematically high (ranging between 66 and 107 cm s^{-1}, on average 92 ± 15 SD cm s^{-1}) during the flux measurements carried out at wind speeds below 4 m s^{-1}. Hence, it is not possible to directly compare k_{600} and water currents.

The k_{600} data set of the Randers Fjord was filtered by rejecting data for wind speeds above 4 m s^{-1} and for nil water currents (Fig. 4). Coincidentally, the k_{600} data are grouped for two wind speed ranges between 0 and 1 m s^{-1} and between 2 and 4 m s^{-1} (Fig. 4A). Even at these low wind speeds, wind stress contributes to k_{600}, as shown by the comparison of the data group for wind speeds below 1 m s^{-1} (filled squares in Fig. 4A) and the data group for wind speed above 2 m s^{-1} and water currents below 10 cm s^{-1} (open squares in Fig. 4A). Thus, the groups of k_{600} data for the two wind speed ranges are treated separately in relation to water currents (Fig. 4B). For the data group for wind speed below 1 m s^{-1}, the range of water currents is low (1 to 8 cm s^{-1}) and no relationship between k_{600} and water current is apparent. However, for the data group of wind speeds between 2 and 4 m s^{-1}, the range of water currents is high (1 to 38 cm s^{-1}) and k_{600} is well related to water current (Fig. 4B). This clearly shows that water currents contribute to k_{600}.

In the Scheldt, a different approach than in the Randers Fjord was used; the contribution of water current to k_{600} was estimated based on the frequently referenced conceptual relationship of O'Connor and Dobbins (1958) that gives the oxygen reaeration rate (R, d^{-1}) according to

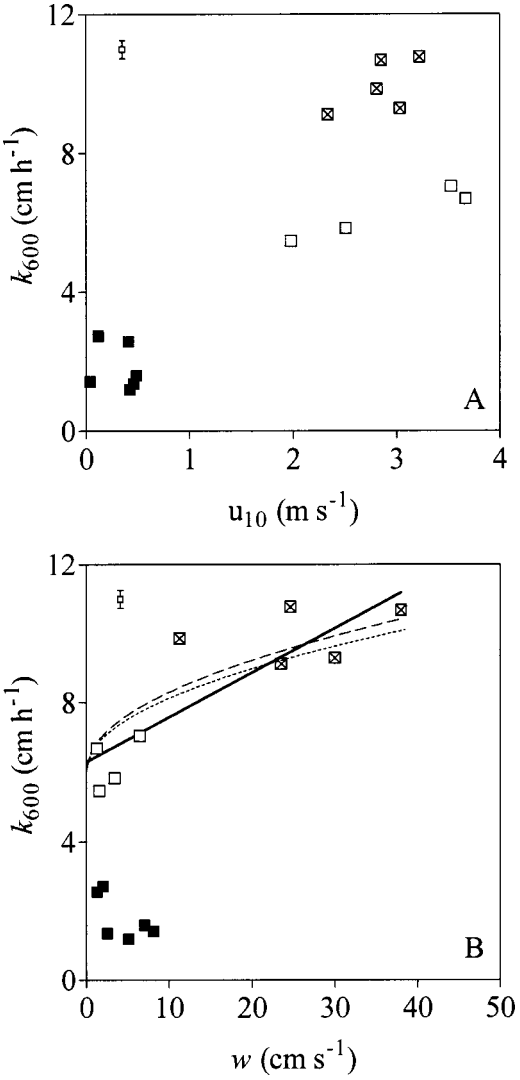

Fig. 4. The gas transfer velocity of CO_2 (k_{600}, cm h^{-1}) in the Randers Fjord as a function of (A) wind speed at 10 m height (u_{10}, m s^{-1}) less than 4 m s^{-1} and (B) non-nil water current (w, cm s^{-1}). The error bars on top left corner of the plots correspond to the average uncertainty on k_{600} (refer to legend of Fig. 2 for details). Filled squares correspond to data below a wind speed of 1 m s^{-1}. For clarity in the data interpretation and discussion, data for wind speeds above 2 m s^{-1} were separated for water currents above (crossed squares) and below (open squares) 10 cm s^{-1}. The short-dashed line corresponds to the k_{600} predicted from the conceptual relationship of O'Connor and Dobbins (1958) to which was added 6.1 cm h^{-1} (a depth 7 m was used in the computation, corresponding to the average value in the navigation channel, where measurements were carried out). The value of 6.1 cm h^{-1} is the average value of the two k_{600} values observed at the lowest (nearly zero) water currents and roughly accounts for the effect of wind speed on k_{600} evident from panel A. The solid line corresponds to the model 1 linear regression ($k_{600} = 6.3$ [±1.1 SE] + 0.13 [±0.03 SE] w, $r^2 = 0.732$, $p = 0.0033$, $n = 9$) between all the observed k_{600} for the wind speed range between 2 and 4 m s^{-1} and water current. The long-dashed line corresponds to a power law function ($k_{600} = 1.87$ [±0.03 SE] $w^{0.5}h^{-0.5}$, $r^2 = 0.725$, $n = 9$) that accounts for w and depth (h, m) in the same fashion as the O'Connor and Dobbins (1958) relationship ($k_{600} = 1.719w^{0.5}h^{-0.5}$), based on all the observed k_{600} for the wind speed range between 2 and 4 m s^{-1}.

$$R = 0.439w^{0.5}h^{-1.5} \quad (2)$$

where w is the water current in centimeters per second and h is the depth in meters.

The oxygen reaeration rate given in Eq. 2 can be expressed as the gas transfer velocity ($k = Rh$) and normalized to a Schmidt number of 600 using the formulations given by Wanninkhof (1992), assuming a dependency of k proportional to $Sc^{-0.5}$, with the result that

$$k_{600\text{current}} = 1.719w^{0.5}h^{-0.5} \quad (3)$$

where $k_{600\text{current}}$ is the gas transfer velocity of CO_2 in centimeters per hour, w is the water current in centimeters per second, and h is the depth in meters.

From the water current measurements concomitant to those of the CO_2 flux, the contribution of water current to the gas transfer velocity of CO_2 ($k_{600\text{current}}$) was computed according to Eq. 3 and was removed from the observed k_{600} ($k_{600\text{observed}}$). This gives in theory the contribution to k_{600} of wind speed alone ($k_{600\text{wind}} = k_{600\text{observed}} - k_{600\text{current}}$), assuming that both contributions to water turbulence are additive. At low wind speeds, $k_{600\text{wind}}$ is about three times lower than $k_{600\text{observed}}$, which suggests that the contribution of water currents to water turbulence is substantial when wind stress is low (Fig. 5A). At high wind speeds, $k_{600\text{wind}}$ is about 1.1 times lower than $k_{600\text{observed}}$, in agreement with the theoretical analysis of Cerco (1989) that shows that the relative contribution of water currents to the gas transfer velocity decreases with increasing wind.

The y-intercept of the model 2 regression function of $k_{600\text{wind}}$ against wind speed for the Scheldt is negative but close to zero (Table 4). This is most probably related to the poor constraint on the linear regression at low wind because only two measurements were obtained for wind speeds below 2 m s^{-1}. The other possible explanation is that the conceptual relationship of O'Connor and Dobbins (1958) overestimates the contribution of water currents to the gas transfer velocity. However, in the Randers Fjord, the curve of k_{600} as a function of w predicted by the O'Connor and Dobbins (1958) relationship (short-dashed line in Fig. 4B; Eq. 3) is close to the regression line of the observed k_{600} as a function of w (solid line in Fig. 4B; $k_{600} = 6.3 + 0.13w$) (Fig. 4B).

A power law function that accounts for w and h in the same fashion as the O'Connor and Dobbins (1958) relationship (short-dashed line in Fig. 4B; Eq. 3) was established from the observed k_{600} and w values (long-dashed line in Fig. 4B; $k_{600} = 1.87w^{0.5}h^{-0.5}$), and both relationships are very similar (Fig. 4B). Zappa et al. (2003) also showed that the O'Connor and Dobbins (1958) relationship gives a good approximation of four k measurements based on the gradient flux technique during a tidal cycle in Plum Island Sound estuary under low wind conditions. Our results and those of Zappa et al. (2003) strongly suggest that the O'Connor and Dobbins (1958) relationship gives a fairly adequate estimation of the contribution of water currents to the gas transfer velocity in estuarine environments.

The same computations as those outlined above were carried out for the Randers Fjord (Fig. 5B and Table 4), and the y-intercepts of the linear regression function of $k_{600\text{observed}}$ and $k_{600\text{wind}}$ against wind speed are not significantly different. This suggests that the overall contribution of water currents to k_{600} is negligible in the microtidal Randers Fjord. Indeed, 78% of the observed water currents are below 10 cm s^{-1} (Fig. 6A) and, thus, the high water currents in Fig. 4B are exceptional values. Moreover, for water currents ranging

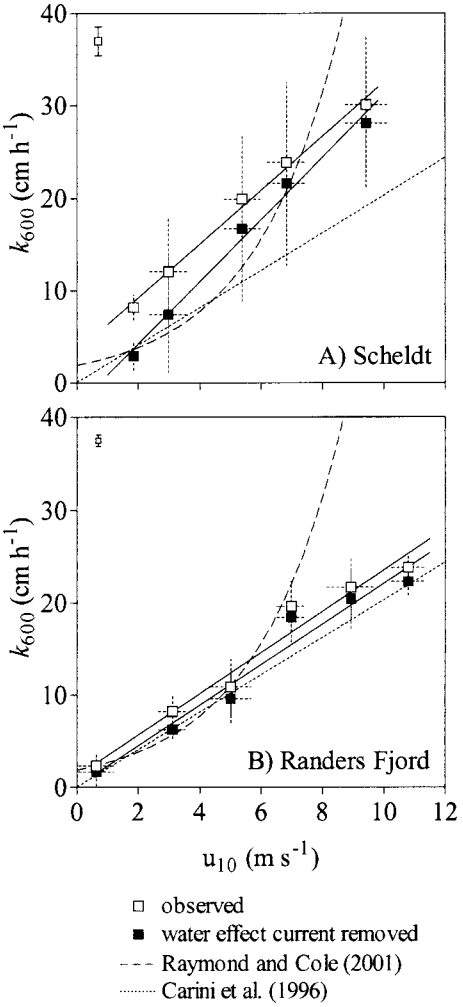

Fig. 5. Gas transfer velocity of CO_2 (k_{600}, cm h^{-1}) as a function of wind speed at 10 m height (u_{10}, m s^{-1}) for (A) the November 2002 Scheldt cruise and (B) for the two Randers Fjord cruises. The data were averaged over wind speed bins of 2 m s^{-1}. Standard deviations are shown by the horizontal and vertical dotted lines for the bin averages of u_{10} and k_{600}, respectively. The error bars on the top left corner of the plots correspond, for each of the two estuaries, to the average uncertainty on k_{600} (refer to legend of Fig. 2 for details). The open symbols correspond to the observed k_{600}. The filled symbols correspond to k_{600} from which the contribution of water currents was removed. The contribution of water currents to k_{600} was estimated from the conceptual relationship of O'Connor and Dobbins (1958), using water current measurements concomitant to the CO_2 flux measurements, and it was removed from individual k_{600} estimates before the data were bin averaged. Solid lines correspond to the model 2 regression functions developed in Table 4. The long-dashed line corresponds to the Raymond and Cole (2001) relationship, and the short-dashed line corresponds to the Carini et al. (1996) relationship (refer to legend of Fig. 2 for details).

Table 4. Regression functions between the gas transfer velocity of CO_2 (k_{600}, cm h^{-1}) and wind speed at 10-m height (u_{10}, m s^{-1}) in the Randers Fjord and the Scheldt (only the data from the November 2002 cruise).*

	$k_{600} = a(\pm SE) + b(\pm SE)u_{10}$	r^2	p	n
Observed k_{600}: unbinned data				
Scheldt	$k_{600} = 4.7(\pm 2.2) + 2.76(\pm 0.33)u_{10}$	0.897	<0.0001	112
Randers Fjord	$k_{600} = 1.2(\pm 0.7) + 2.30(\pm 0.11)u_{10}$	0.395	<0.0001	56
k_{600} without the contribution from water currents: unbinned data				
Scheldt	$k_{600} = -0.8(\pm 2.3) + 3.16(\pm 0.34)u_{10}$	0.898	<0.0001	112
Randers Fjord	$k_{600} = 0.1(\pm 0.6) + 2.26(\pm 0.10)u_{10}$	0.439	<0.0001	56
Observed k_{600}: binned data				
Scheldt	$k_{600} = 3.4(\pm 0.8) + 2.92(\pm 0.14)u_{10}$	0.993	0.0005	5
Randers Fjord	$k_{600} = 0.9(\pm 1.5) + 2.30(\pm 0.22)u_{10}$	0.963	0.0002	6
k_{600} without the contribution from water currents: binned data				
Scheldt	$k_{600} = -2.7(\pm 1.2) + 3.41(\pm 0.21)u_{10}$	0.989	0.0006	5
Randers Fjord	$k_{600} = -0.3(\pm 1.6) + 2.28(\pm 0.24)u_{10}$	0.959	0.0005	6

* For unbinned data, the regression function was computed with model 1 least-squares fit. For bin-averaged data, the regression function was computed with model 2 functional fit. The contribution of water currents to k_{600} was estimated from the conceptual relationship of O'Connor and Dobbins (1958), using water current measurements concomitant to those of air–water CO_2 fluxes. This contribution was removed from the observed individual k_{600}, and data were then averaged over wind speed bins of 2 m s^{-1} and the model 2 regression functions against u_{10} were recomputed (lower half of table). In the Scheldt, for the regression functions of the observed k_{600} and the k_{600} without the contribution from water currents, the slopes are not statistically different ($p = 0.3881$ for unbinned data; $p = 0.1059$ for binned data) but the y-intercepts are statistically different ($p = 0.0052$ for unbinned data; $p = 0.0028$ for binned data). In the Randers Fjord, for the regression functions of the observed k_{600} and the k_{600} without the contribution from water currents, the slopes ($p = 0.8015$ for unbinned data; $p = 0.9164$ for binned data) and the y-intercepts ($p = 0.0133$ for unbinned data; $p = 0.2263$ for binned data) are not statistically different.

from 0 to 10 cm s^{-1}, the expected increase of k_{600} is on average only of a factor of about 1.2, based on the linear regression function in Fig. 4B. Also, the k_{600} data of the Randers Fjord follow closely the relationship of Carini et al. (1996) for Parker River estuary (Figs. 2, 3, and 5B) that is also characterized by low tidal currents according to Raymond and Cole (2001).

In contrast, 67% of the observed water currents in the Scheldt estuary are above 10 cm s^{-1}, and the range of variation of the observed water currents is higher than in the Randers Fjord (Fig. 6B). This supports the idea that the difference in the y-intercept of the regression functions of k_{600} against wind speed between the Randers Fjord and the Scheldt (Table 3) is related to the contribution of water currents to k_{600} that is substantial in the Scheldt and negligible in the Randers Fjord. This is also consistent with the low y-intercept of the regression function of k as a function of wind speed reported by Kremer et al. (2003*a*) for Childs River and Sage Lot Pond estuaries (respectively, 1.9 and 0.8 cm h^{-1} normalized to a Sc of 600) that are close to the value in Randers Fjord. Indeed, Waquoit Bay is characterized by a low tidal amplitude (<0.5 m); thus, tidal currents can be assumed to be low in Childs River and Sage Lot Pond estuaries and, according to Kremer et al. (2003*a*), have a negligible effect on k. The high y-intercept of the regression functions of k_{600} against wind speed of the Thames (Table 3) is also assumed to be related to strong tidal currents, although no water current measurements are available to verify this hypothesis. The high tidal amplitude in the Thames (Table 1) suggests that tidal currents should be at least as strong as in the Scheldt.

Fetch limitation?—In addition to the differences in y-intercepts, the regression functions of k_{600} against wind speed of the Scheldt and the Thames have higher slopes compared to the one of the Randers Fjord (Table 3). This is not related to water currents because their contribution to k_{600} tends on the contrary to slightly decrease the slope (Fig. 5A; Table 4). This difference could be related to fetch limitation. Fetch is the distance over which the wind blows without significant deviation and determines (for a given wind speed) the intensity of water turbulence and wave height. The effect of fetch on k has been shown in wind tunnel experiments (Wanninkhof and Bliven 1991). Hartman and Hammond (1984) suggested fetch limitation to explain the differences of k values on the different sides of San Francisco Bay. Kremer et al. (2003*a*) have hypothesized that the lower slopes of k–wind linear relationships in Sage Lot Pond and Childs River compared to other estuaries could be related to fetch limitation. Also, Wanninkhof (1992) hypothesized that the difference between the slope of the linear regression functions of k_{600} (based on SF_6 evasion experiments) against wind speed in various lakes is related to their surface area.

Among the three studied estuaries, the Randers Fjord is shorter and narrower and has a smaller surface area than the Scheldt and Thames (Table 1). Thus, stronger fetch limitation could explain the lower slope of the linear regression function of k_{600} against wind in the Randers Fjord compared to the other two estuaries. In Fig. 7, the slopes of the regression functions of the three studied estuaries plus those investigated by Kremer et al. (2003*a*) are plotted on a semilogarithmic scale against their respective estuarine surface area. This clearly shows a significant effect of fetch limita-

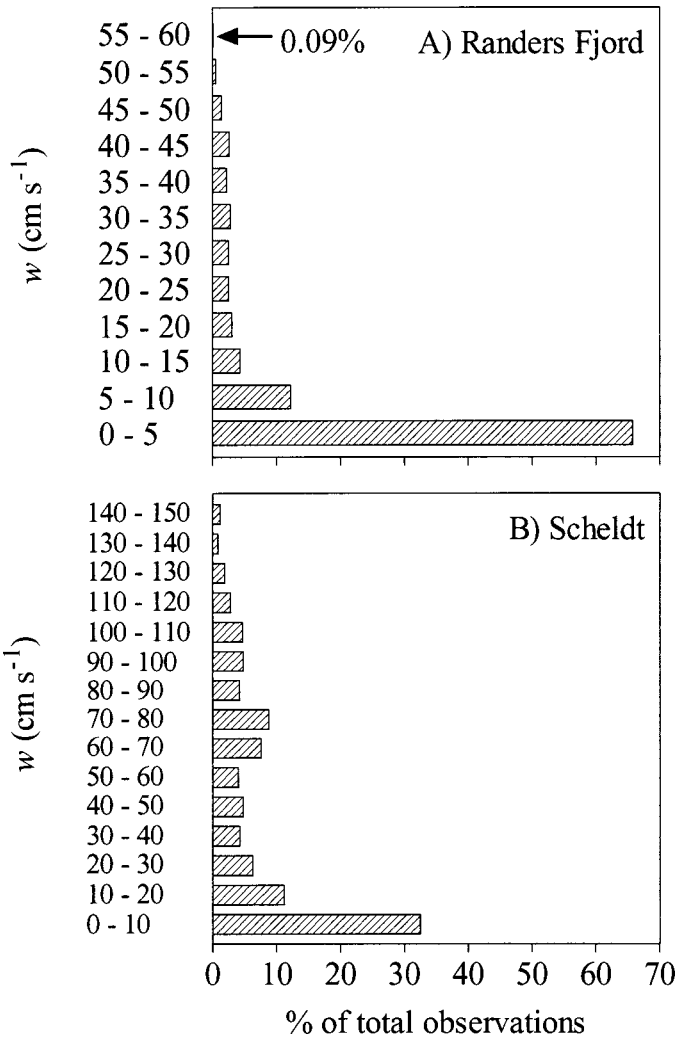

Fig. 6. Frequency distribution of water current (w, cm s^{-1}) measurements by (A) intervals of 5 cm s^{-1} in the Randers Fjord (total number of observations = 7,909) and by (B) intervals of 10 cm s^{-1} in the Scheldt (total number of observations = 2,278). During both Randers Fjord cruises, data were recorded every minute at three stations (56.46°N 10.04°E, 56.62°N 10.23°E, 56.61°N 10.30°E) that were occupied during 24 h. Data at the upstream station (56.46°N 10.04°E) were lost because of equipment failure during the April 2001 cruise. During the November 2002 Scheldt cruise, data were recorded every minute at four stations (51.13°N 4.31°E, 51.23°N 4.40°E, 51.41°N 4.04°E, 51.39°N 4.21°E) that were occupied during 24 h. Mean current speeds are 8 (±12 SD) and 44 (±40 SD) cm s^{-1} in the Randers Fjord and the Scheldt, respectively.

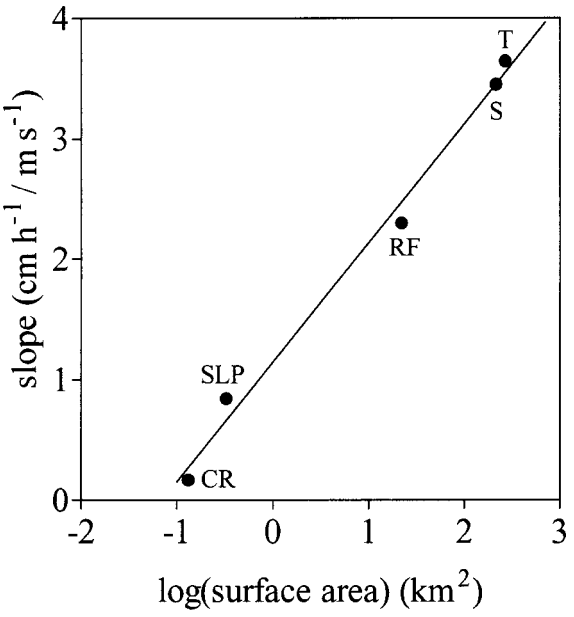

Fig. 7. Slope of the model 1 regression functions of k_{600} versus wind speed (Table 3) from the Thames (T), Scheldt (S), Randers Fjord (RF), Childs River (CR), and Sage Lot Pond (SLP) versus the logarithm of the estuarine surface area. The data from Childs River (1.3 km^2) and Sage Lot Pond (3.3 km^2) from Kremer et al. (2003*a*) were normalized to a Schmidt number of 600 using the formulations given by Wanninkhof (1992) and assuming a dependency of the gas transfer velocity proportional to $Sc^{-0.5}$. Solid line corresponds to model 1 regression function (slope = 1.14 (±0.09 SE) + 0.99 (±0.05 SE) log (surface area), $r^2 = 0.991$, $p = 0.0003$, $n = 5$).

tion on k that induces a decrease of the slope of the k versus wind speed regression functions with increasing fetch limitation. The nonlinearity of the relationship suggests that the effect of fetch limitation is disproportionately stronger in small estuaries (<30 km^2). However, Fig. 7 should be interpreted with caution since besides the estuarine surface area, fetch limitation is expected to depend on the shape of the estuary (funnel, oval, narrow or wide linear channel) and on the relation between the direction of prevailing winds and the direction of main axis of the estuary (parallel or across).

When compared at the European regional level, the integrated air–water CO_2 fluxes in estuaries and open continental shelf are of the same order of magnitude but opposite in direction. Thus, more air–water CO_2 flux estimates are needed in worldwide estuaries to allow an evaluation of their significance in the CO_2 flux budget of the overall coastal ocean. The critical factor in the computation of the air–water CO_2 flux is the large uncertainty on the formulation of the gas transfer velocity. Based on a fairly large data set of air–water CO_2 fluxes, measured using the floating chamber method, in three European estuaries (Randers Fjord, Scheldt, and Thames), significant regression functions between k_{600} and wind speed were established. Based on these and in accordance with the conclusions of Kremer et al. (2003*a*), it appears that the formulation of k_{600} as a function of wind speed is site specific in estuarine environments. This implies that substantial errors in flux computations are incurred if generic k–wind relationships are employed in estuarine environments for the purpose of biogas air–water flux budgets and ecosystem metabolic studies. From one estuary to another, the differences in the y-intercepts of the linear relationships are due to tidal currents, whereas the differences in the slopes of the regression functions are related to fetch limitation. The contribution of tidal currents to k_{600} is significant in macrotidal estuaries such as the Scheldt and Thames but seems negligible in microtidal estuaries such as Randers Fjord, Childs River, and Sage Lot Pond. Based on our results and in accordance with those of Zappa et al.

(2003), the O'Connor and Dobbins (1958) relationship originally developed for streams is appropriate to estimate the contribution of waters currents to k in estuarine environments. Finally, we suggest that in estuarine environments future research efforts should concentrate in the development of a physically more rigorous and probably multivariable formulation of the gas transfer velocity (including at least wind stress and water current effects on turbulence at the air–water interface), rather than a simple empirical formulation as a function of wind speed. To assist such theoretical work, more data on air–water CO_2 fluxes are also needed. Natural or purposeful tracer approaches give gas transfer velocity estimates that are on a time scale (day to week) that is larger than the one characteristic of tidal currents (minutes to hours). To resolve gas transfer velocity variability on short time scales, besides the floating chamber method, micrometeorological methods seem adequate. The earlier controversial drawbacks of these methods (Broecker et al. 1986) seem to a large extent resolved (Fairall et al. 2000; McGillis et al. 2001), and estuaries provide ideal settings for their application (low ship motion, high signal-to-noise ratio, i.e., very large fluxes and ΔpCO_2).

References

BAKKER, D. C. E., H. J. W. DE BAAR, AND H. P. J. DE WILDE. 1996. Dissolved carbon dioxide in Dutch coastal waters. Mar. Chem. **55:** 247–263.

BANSAL, M. K. 1973. Atmospheric reaeration in natural streams. Water Res. **7:** 769–782.

BELANGER, T. V., AND E. A. KORZUM. 1991. Critique of floating-dome technique for estimating reaeration rates. J. Environ. Eng. **117:** 144–150.

BORGES, A. V., AND M. FRANKIGNOULLE. 2001. Short-term variations of the partial pressure of CO_2 in surface waters of the Galician upwelling system. Prog. Oceanogr. **51:** 283–302.

———, AND ———. 2002*a*. Distribution of surface carbon dioxide and air-sea exchange in the upwelling system off the Galician coast. Glob. Biogeochem. Cycles **16:** 1–14.

———, AND ———. 2002*b*. Distribution and air-water exchange of carbon dioxide in the Scheldt plume off the Belgian coast. Biogeochemistry **59:** 41–67.

BROECKER, H. C., AND W. SIEMS. 1984. The role of bubbles for gas transfer from water to air at higher wind speeds: Experiments in wind-wave facility in Hamburg, p. 229–238. *In* W. Brutsaert and G. H. Jirka [eds.], Gas transfer at water surfaces. Reidel.

BROECKER, W. S., J. R. LEDWELL, T. TAKAHASHI, L. M. R. WEISS, L. MEMERY, T.-H. PENG, B. JÄHNE, AND K. O. MÜNNICH. 1986. Isotopic versus micrometeorologic ocean CO_2 fluxes: A serious conflict. J. Geophys. Res. **91:** 10517–10527.

CAI, W.-J., Z. H. A. WANG, AND Y. C. WANG. 2003. The role of marsh-dominated heterotrophic continental margins in transport of CO_2 between the atmosphere, the land-sea interface and the ocean. Geophys. Res. Lett. **30:** 1849, doi:10.1029/2003GL017633

———, W. J. WIEBE, Y. WANG, AND J. E. SHELDOM. 2000. Intertidal marsh as a source of dissolved inorganic carbon and a sink of nitrate in the Satilla River-estuarine complex in the southeastern U.S. Limnol. Oceanogr. **45:** 1743–1752.

CARINI, S., N. WESTON, C. HOPKINSON, J. TUCKER, A. GIBLIN, AND J. VALLINO. 1996. Gas exchange rates in the Parker River estuary, Massachusetts. Biol. Bull. **191:** 333–334.

CERCO, C. F. 1989. Estimating estuarine reaeration rates. J. Environ. Eng. **115:** 1066–1070.

COLE, J. J., AND N. F. CARACO. 1998. Atmospheric exchange of carbon dioxide in a low-wind oligotrophic lake measured by the addition of SF_6. Limnol. Oceanogr. **43:** 647–656.

DEGRANPRE, M. D., G. J. OLBU, C. M. BEATTY, AND T. R. HAMMAR. 2002. Air-sea fluxes on the US Middle Atlantic Bight. Deep-Sea Res. II **49:** 4355–4367.

FAIRALL, C. W., J. E. HARE, J. B. EDSON, AND W. MCGILLIS. 2000. Parameterization and micrometeorological measurement of air-sea gas transfer. Boundary-Layer Meteorol. **96:** 63–105.

FRANKIGNOULLE, M. 1988. Field measurements of air-sea CO_2 exchange. Limnol. Oceanogr. **33:** 313–322.

———, G. ABRIL, A. BORGES, I. BOURGE, C. CANON, B. DELILLE, E. LIBERT, AND J.-M. THÉATE. 1998. Carbon dioxide emission from European estuaries. Science **282:** 434–436.

———, R. BIONDO, J.-M. THÉATE, AND A. V. BORGES. 2003. Carbon dioxide daily variations and atmospheric fluxes over the open waters of the Great Bahama Bank and Norman's Pond using a novel autonomous measuring system. Caribb. J. Sci. **39:** 257–264.

———, AND A. V. BORGES. 2001*a*. European continental shelf as a significant sink for atmospheric CO_2. Glob. Biogeochem. Cycles **15:** 569–576.

———, AND ———. 2001*b*. Direct and indirect pCO_2 measurements in a wide range of pCO_2 and salinity values (The Scheldt Estuary). Aquat. Geochem. **7:** 267–273.

———, ———, AND R. BIONDO. 2001. A new design of equilibrator to monitor carbon dioxide in highly dynamic and turbid environments. Water Res. **35:** 1344–1347.

———, J.-P. GATTUSO, R. BIONDO, I. BOURGE, G. COPIN-MONTÉGUT, AND M. PICHON. 1996. Carbon fluxes in coral reefs. II. Eulerian study of inorganic carbon dynamics and measurement of air-sea CO_2 exchanges. Mar. Ecol. Prog. Ser. **145:** 123–132.

GATTUSO, J.-P., M. FRANKIGNOULLE, AND R. WOLLAST. 1998. Carbon and carbonate metabolism in coastal aquatic ecosystems. Annu. Rev. Ecol. Syst. **29:** 405–433.

GUALTIERI, C., P. GUALTIERI, AND G. P. DORIA. 2002. Dimensional analysis of reaeration rate in streams. J. Environ. Eng. **128:** 12–18.

HARTMAN, B., AND D. H. HAMMOND. 1984. Gas exchange across the sediment-water and air-water interfaces in south San Francisco Bay. J. Geophys. Res. **89:** 3593–3603.

———, AND ———. 1985. Gas exchange in San Francisco Bay. Hydrobiologia **129:** 59–68.

JACOBS, C. M. J., W. KOHSIEK, AND W. A. OOOST. 1999. Air-sea fluxes and transfer velocity of CO_2 over the North Sea: Results from ASGAMAGE. Tellus **51B:** 629–641.

KREMER, J. N., A. REISCHAUER, AND C. D'AVANZO. 2003*a*. Estuary-specific variation in the air-water gas exchange coefficient for oxygen. Estuaries **26:** 829–836.

———, S. W. NIXON, B. BUCKLEY, AND P. ROQUES. 2003*b*. Technical note: Conditions for using the floating chamber method to estimate air-water gas exchange. Estuaries **26:** 985–990.

LISS, P. S., AND L. MERLIVAT. 1986. Air-sea exchange rates: introduction and synthesis, p. 113–127. *In* P. Buat-Ménard [ed.], The role of air-sea exchange in geochemical cycling. Reidel.

MARINO, R., AND R. W. HOWARTH. 1993. Atmospheric oxygen exchange in the Hudson river: Dome measurements and comparison with other natural waters. Estuaries **16:** 433–445.

MATTHEWS, C. J. D., V. L. ST. LOUIS, AND R. H. HESSLEIN. 2003. Comparison of three techniques used to measure diffusive gas exchange from sheltered aquatic surfaces. Environ. Sci. Technol. **37:** 772–780.

MCGILLIS, W. R., J. B. EDSON, J. D. WARE, J. W. H. DACEY, J. E. HARE, C. W. FAIRALL, AND R. WANNINKHOF. 2001. Carbon

dioxide flux techniques performed during GasEx-98. Mar. Chem. **75:** 267–280.

MELCHING, C. S., AND H. E. FLORES. 1999. Reaeration equations derived from U.S. Geological Survey Database. J. Environ. Eng. **125:** 407–414.

NIGHTINGALE, P. D., G. MALIN, C. S. LAW, A. J. WATSON, P. S. LISS, M. I. LIDDICOAT, J. BOUTIN, AND R. C. UPSTILL-GODDARD. 2000. In situ evaluation of air-sea exchange parameterizations using novel conservative and volatile tracers. Glob. Biogeochem. Cycles **14:** 373–387.

O'CONNOR, D. J., AND W. E. DOBBINS. 1958. Mechanism of reaeration in natural streams. Trans. Am. Soc. Civ. Eng. **123:** 641–684.

RAYMOND, P. A., J. E. BAUER, AND J. J. COLE. 2000. Atmospheric CO_2 evasion, dissolved inorganic carbon production, and net heterotrophy in the York River estuary. Limnol. Oceanogr. **45:** 1707–1717.

———, AND J. J. COLE. 2001. Gas exchange in rivers and estuaries: Choosing a gas transfer velocity. Estuaries **24:** 312–317.

SMITH, S. D. 1988. Coefficients for sea surface wind stress, heat flux, and wind profiles as a function of wind speed and temperature. J. Geophys. Res. **93:** 15467–15472.

SMITH, S. V., AND G. S. KEY. 1975. Carbon dioxide and metabolism in marine environments. Limnol. Oceanogr. **20:** 493–495.

———, AND F. T. MACKENZIE. 1987. The ocean as a net heterotrophic system: Implications from the carbon biogeochemical cycle. Glob. Biogeochem. Cycles **1:** 187–198.

TSUNOGAI, S., S. WATANABE, AND T. SATO. 1999. Is there a ''continental shelf pump'' for the absorption of atmospheric CO_2? Tellus **51B:** 701–712.

WANNINKHOF, R. 1992. Relationship between wind speed and gas exchange over the ocean. J. Geophys. Res. **97:** 7373–7382.

———, AND L. BLIVEN. 1991. Relationship between gas exchange, wind speed and radar backscatter in large wind-wave tank. J. Geophys. Res. **96:** 2785–2796.

———, AND W. R. MCGILLIS. 1999. A cubic relationship between air-sea CO_2 exchange and wind speed. Geophys. Res. Lett. **26:** 1889–1892.

WEISS, R. F. 1974. Carbon dioxide in water and seawater: The solubility of a non-ideal gas. Mar. Chem. **2:** 203–215.

ZAPPA, C. J., P. A. RAYMOND, E. A. TERRAY, AND W. R. MCGILLIS. 2003. Variation in surface turbulence and the gas transfer velocity over a tidal cycle in a macro-tidal estuary. Estuaries **26:** 1401–1415.

Received: 3 November 2003
Amended: 14 May 2004
Accepted: 17 May 2004